

A Broadband CPW-FCL Gyrator

Mahmoud A. Abdalla^{1, *} and Zhirun Hu²

Abstract—In this paper, a novel wideband gyrator based on a ferrite coupled line design approach and realized in coplanar waveguide configuration is presented. The ferrite coupled lines are proved to demonstrate typical unique properties. The design of the optimum coupled lines has shown an almost 1 dB/3 dB insertion loss for even/odd modes excitation respectively. Also, for single excitation, the power is divided at output ports with insertion loss almost equal to 3 dB and 5 dB, good matching and isolation between output ports (less than -15 dB). The bandwidth of the designed coupler is proved over the bandwidth of 7 GHz–11 GHz. As an application, a novel gyrator is introduced and covers the same coupler bandwidth. The performance of the gyrator is optimized using full-wave simulations.

1. INTRODUCTION

The need for modern microwave components with nonreciprocal properties is a continuous demand for simultaneous-transmit-and-receive (STAR) systems such as modern wireless systems and radar systems that keep research hot topic [1–3]. The designs of microwave components have utilized different approaches such as Faraday Rotation (propagation along the magnetization direction), ferromagnetic resonance, and field displacement (for propagation normal to the magnetization direction) [4]. As a result, intensive design for nonreciprocal magnetic components such as an isolator, gyrators, circulators, tunable filters, high-power switches, and non-reciprocal phase shifters have been presented [5–8].

Conventional nonreciprocal devices have been designed using transversely magnetized traditional junction structures [9–11]. However, these components have many drawbacks. First, the design of nonreciprocal devices is mainly dependent on the wavelength which results in bulky devices at low frequencies at microwave bands and also too small structures to be manufactured in cheap technology at millimeter waves. Second, the normal magnetization direction will have a large demagnetization factor hence will need to apply a high DC magnetic bias field which in return needs high cooling systems strong biasing magnetic field. Finally, due to the previous conditions and also due to the limitation of magnetization saturation of the available ferrites, the conventional junction nonreciprocal components have narrow bands, especially at high millimeter waves [6, 7].

In literature, different approaches have been proposed to find solutions for the previous limitations. One solution is using hexaferrite (self-biased ferrites), which are ferrite materials used as permanent magnets, and hence they do not require high magnetization. They have been applied in different components such as circulators [12, 13] and isolators [14]. Also, using ferromagnetic nanowires has been employed as other self-biased ferrites and applied in circulator design [15, 16]. Using a new planar configuration such as a substrate integrated waveguide can handle the problem of high insertion loss for isolators [17, 18] and also circulators [19, 20]. The narrow bandwidth of the ferrite components has been addressed using another approach such as the edge-guided mode for ferrite nonreciprocal circuits, which can also introduce high non-reciprocity [21, 22].

Received 21 April 2019, Accepted 14 July 2022, Scheduled 26 July 2022

* Corresponding author: Mahmoud Abdelrahman Abdalla (maaabdallah@mtc.edu.eg).

¹ Department of Electronic Engineering, Military Technical College, El-Qobba Bridge, Cairo. ² School of Electrical & Electronic Engineering, University of Manchester, UK.

Using a coplanar waveguide (CPW) has many advantages. First, it is compatible with MMIC circuits, and second, it needs a small demagnetization factor, which means that no strong DC magnetic bias is needed. Examples of many nonreciprocal CPW couplers, isolators, and circulators have been presented in [23–27]. However, no gyrator is presented in CPW configuration given the importance of the gyrator function to planar MMIC circuits and especially in transmitting-receiving applications.

In the past years, using ferrite coupled lines (FCLs) has been presented as a new design approach that applies longitudinal magnetization for ferrite substrate, and hence, it has **solved** the problem of size constraints, losses at millimeter waves in addition to the non-strong needed magnetic bias without the need of self-biased ferrites (low-cost conventional lithium or YIG ferrites) and also the possibility of broad bandwidth. The first FCL experimental realization was in finline configuration [28]. Next, it was presented in microstrip configuration [29, 30] with applications of isolators [31, 32] and circulator [33]. Also, FCL was realized in stripline configuration [34] with circulator applications [35, 36]. FCL was presented as a slotline configuration [37]. In CPW configuration, FCL was proposed in [38] and applied in the circulator [39]. There is a continuous demand for FCL new configurations [40–42]. Coupled mode approach [43, 44] and normal mode approach [45–47] have been used to give a theoretical explanation for FCL performance.

In previous work in literature, there have been limited FCL gyrator applications [48, 49], and up to the authors' knowledge, no CPW-FCL-based gyrator is presented. In this paper, the design and simulation of broadband CPW-FCL are presented. As an application of the proposed designed FCL junction, an FCL gyrator has been introduced. This paper is divided into two main parts. The first part introduces the CPW-FCL section, and the second one introduces the CPW-FCL gyrator. Detailed theoretical basis and EM full-wave simulations are discussed.

2. CPW-FCL

2.1. CPW-FCL Theory

The FCL concept is based on longitudinally magnetizing two parallel and coupled transmission lines in planar configurations. The FCL concept is realized in this work as an open CPW one for ease of integration with other microwave components. The detailed cross-section and top view of the CPW-FCL structure are shown in Fig. 1 and Fig. 2 whereas the full 2D layout is plotted in Fig. 3. The two coupled lines are printed on a ferrite substrate. The used ferrite substrate is the commercial YIG Canary Tec. Co. G-113* whose parameters are: (1) the dielectric constant is $\epsilon_f = 15$; (2) the loss tangent is $\tan \delta < 0.0002$; (3) the saturation magnetization is $4\pi M_S = 1780$ Gauss; (4) the magnetic linewidth is $\Delta H_0 \leq 25$ Oe; and (5) the substrate thickness is $d = 1$ mm.

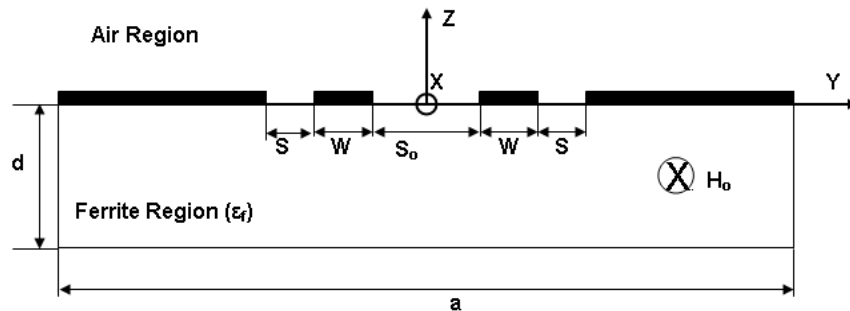


Figure 1. The cross-section of the CPW-FCL junction, $d = 1$ mm.

In Fig. 3, the two coupled lines are fed to $50\ \Omega$ external feeding ports on a dielectric substrate with the same dielectric constant as the ferrite substrate, which is longitudinally magnetically saturated with (H_0) zero DC applied in the longitudinal directions (along X direction) as shown in the figures. Thus,

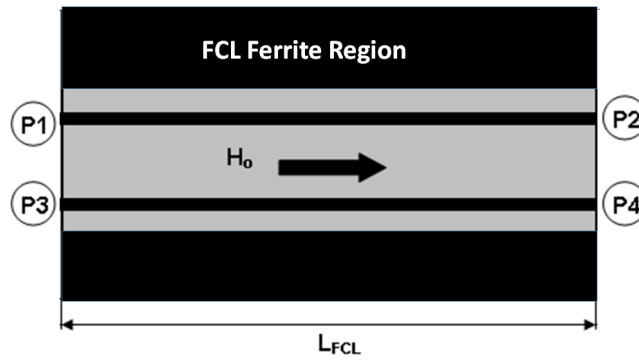


Figure 2. The top view of the CPW-FCL junction.

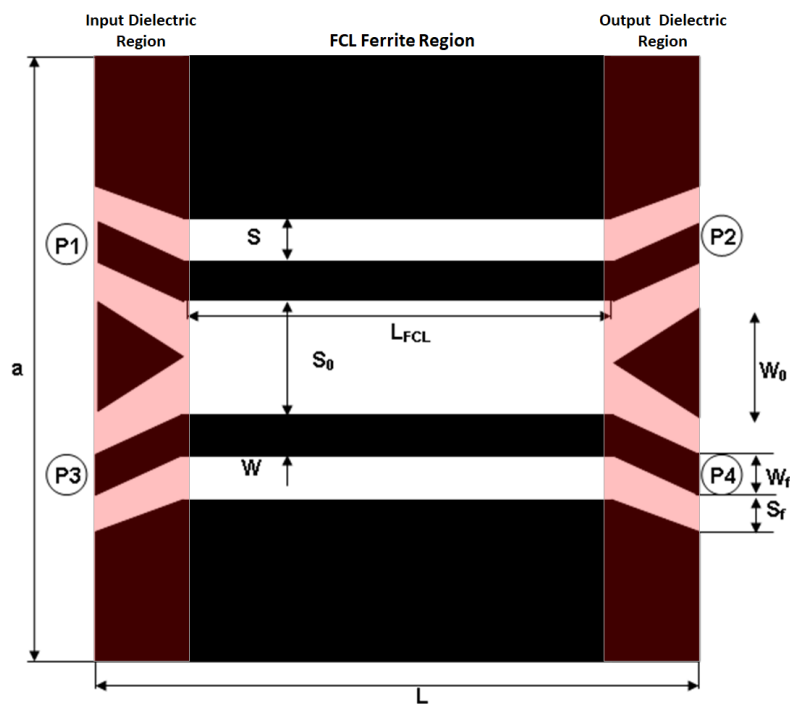


Figure 3. The 2D layout diagram of the CPW-FCL, $a = 4.7$ mm, $L = 39$ mm, $L_{FCL} = 36$ mm, $W = 0.25$ mm, $S = 0.25$ mm, $S_0 = 0.7$ mm, $W_0 = 1.5$ mm, $W_f = 0.25$ mm, $S_f = 0.25$ mm.

the ferrite permeability tensor, $[\mu]$, is [4]

$$[\mu] = \begin{bmatrix} 1 & 0 & 0 \\ 0 & \mu & jk \\ 0 & -jk & \mu \end{bmatrix} \quad (1a)$$

$$\mu = \frac{\omega_{hm}^2 - \omega^2}{\omega_h^2 - \omega^2} \quad (1b)$$

$$k = \frac{\omega\omega_m}{\omega_h^2 - \omega^2}, \quad (1c)$$

$$\omega_h = \mu_o\gamma H_o, \quad \omega_{hm} = \mu_o\gamma\sqrt{H_o(H_o + M_o)}, \quad \omega_m = \mu_o\gamma M_o \quad (1d)$$

where μ_o is the free space permeability, and γ is the ferrite gyromagnetic ratio. Also, the CPW-FCL

effective permeability can be expressed as [49]

$$\mu_{eff} = \frac{(\omega_h + \omega_m)^2 - \omega^2}{\omega_{hm}^2 - \omega^2} \quad (2)$$

The design of the CPW-FCL section is based on assigning the optimum length for the given separation. This design can be achieved with the help of the coupled mode theory. The length is specified such that the coupling between the even- and odd-modes of the unmagnetized symmetric CPW structure is multiple of 45° as

$$CL = \frac{\pi}{4} + \frac{n\pi}{4}, \quad n = 0, 1, 2, \quad (3)$$

where C is the coupling factor caused by the ferrite gyrotropy defined as in (4) [43, 44]

$$C = k_o \eta_o \kappa \int_{\Omega} [\bar{H}_{te} x \bar{H}_{to}^*] \cdot \hat{a}_z d\Omega \quad (4)$$

where k_o and η_o are the free space wave number and intrinsic impedance, respectively, while κ is the off-diagonal element of the permeability tensor, and \hat{a}_z is the direction of propagation. The components H_{te} and H_{to} represent the tangential components of the even and odd modes of the isotropic and non-magnetized ferrite waveguide, respectively. These components are obtained by solving the coupled mode equations in the basic guide. The integration is done over the ferrite region (Ω), where the coupling is assumed to be within and where the transverse components of even and odd modes are perpendicular to each other.

Also, the CPW-FCL section length can be designed by applying the normal mode concept. The optimum length is specified such that the phase of the two propagating dominant normal modes is 90° (the two modes are orthogonal) [45, 46] as in (5)

$$(\beta_1 - \beta_2) L = \frac{\pi}{2} + n\pi, \quad n = 0, 1, 2, \dots \quad (5)$$

where β_1 and β_2 are the propagation constant of the two normal modes which can be obtained by solving the propagating electromagnetic wave equation along with the FCL in terms of its magnetic field H that can be derived using Maxwell's equations as explained in [44] as,

$$\nabla x (\varepsilon^{-1} \nabla x H) - \frac{\omega^2}{c^2} [\mu] H = 0 \quad (6)$$

According to the two different approaches to exploring the performance of the CPW-FCL, it can be proved that the FCL has a nonreciprocal phase shift. In other words, at optimum conditions, the CPW-FCL scattering matrix is written as [38]

$$[S] = \frac{1}{\sqrt{2}} \begin{bmatrix} 0 & 1 & 0 & -1 \\ 1 & 0 & -1 & 0 \\ 0 & 1 & 0 & 1 \\ 1 & 0 & 1 & 0 \end{bmatrix} \quad (7)$$

To satisfy a wideband of operations, this scattering matrix should be satisfied over a wide frequency band. In our work, the wideband ε CPW-FCL has been length optimized to demonstrate the function in the frequency range from 5 GHz to 11 GHz.

2.2. CPW-FCL EM Simulation Results

Based on initial calculations using (3) and (5) for the FCL length, as a guideline, the optimum CPW-FCL junction satisfying the required wideband was obtained through intensive parametric tuning. Finally, the FCL optimum length was set to 36 mm. The commercial software ANSYS-Electronic Desktop was employed.

The simulated scattering parameter magnitudes of the CPW-FCL junction are plotted in Fig. 4. It is shown that the structure reacts as a forward coupler whose scattering transmission coefficient S_{41} is better than -4 dB, and also S_{21} is better than -6 dB in the frequency band from 7 GHz to 11 GHz

with reflection loss S_{11} and isolation loss S_{31} both less than -15 dB. By exciting port (3), similar results can be achieved. As a consequence, it can be claimed that the achieved results confirm the typical FCL magnitude properties.

To confirm the amplitude properties, the same structure was simulated with a dielectric substrate having the same electric permittivity ($\epsilon_r = 15$) and loss tangent ($\tan \delta < 0.0002$) as the previously used ferrite substrate. However, the magnetic properties are different, so they are not the same. The simulated scattering parameter magnitudes for input at port (1) are shown in Fig. 5. The results are different from those shown in Fig. 4. The through power (expressed in terms of S_{21} magnitude) is dominant with a value close to 0 dB, whereas the power at port (4) (expressed in terms of S_{41} magnitude) is at the level of -20 dB.

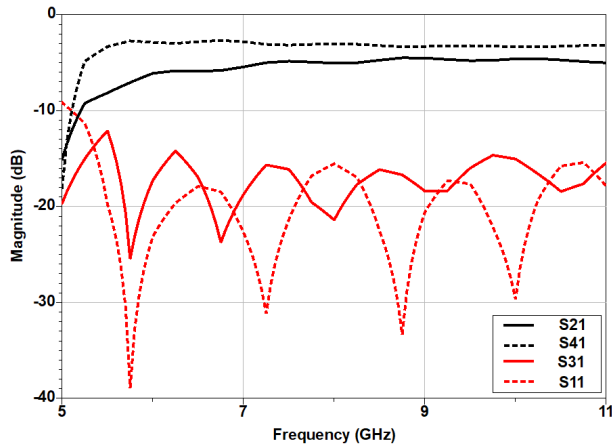


Figure 4. The full-wave simulated magnitude of scattering parameters of the CPW-FCL for input port 1.

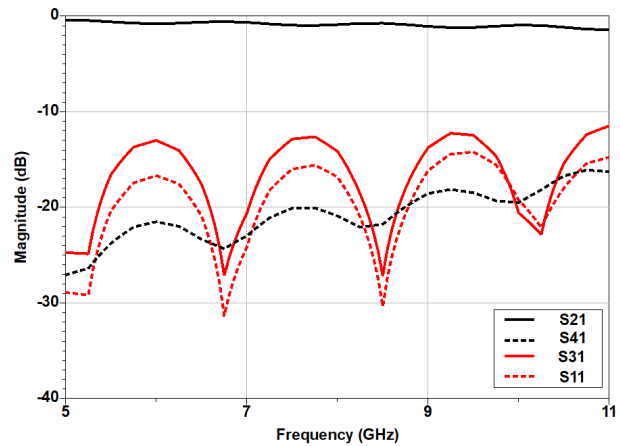


Figure 5. The full-wave simulated magnitude of scattering parameters of the CPW dielectric coupled line for input port 1.

For more emphasizing the proposed FCL structure performance, the phase difference between the two outputs for two excitations: (1) at port 1 as the first case and (2) at port 3 as the second case is plotted in Fig. 6. The phase difference for excitation cases at ports 1 and 3 has a periodic nature. For the case that the excitation is at port 3, the phase difference varies around 0° with a variation that does not exceed 15° in the frequency band up to 10 GHz. For the case where the excitation is at port 1, the phase difference varies around 180° with a variation of a maximum of 10° for the frequency > 6 GHz. This phase's previous results with the approximate power division of the forward coupler confirmed the even/odd modes output on changing the excitation port of the FCL junction, which is a unique property of the FCL junction.

Another verification for the FCL functionality is achieved by exciting the FCL in three cases: (1) At port (1) and hence phase of (S_{21}) and Phase (S_{41}) are extracted. (2) At Port (4) and then phase (S_{14}) is extracted. (3) Excitation at port (2) and hence phase of (S_{12}) is extracted. Next, comparing the phase difference for the reciprocal input at port (1) and port (4), respectively, (phase (S_{41})-phase (S_{14})) to that at port (1) and port (2), respectively, (phase (S_{21})-phase (S_{12})). This comparison is plotted in Fig. 7, where it can be seen that the phase difference (phase (S_{21})-phase (S_{12})) = 0° , which is reciprocal. On the other hand, the phase difference (phase (S_{41})-phase (S_{14})) is 180° .

Moreover, to prove the FCL performance, the even and odd mode excitations have been studied and plotted in Fig. 8. For the odd mode excitation, the output power appears at port 2 with approximately -3 dB level from frequency > 5.5 GHz while it goes to port 4 in the case of the even mode excitation with approximately -1 dB level from frequency > 7 GHz. It is also clear that these two responses have periodic nature (Except S_{4e} where it is not clear). All the previous results completely agree with the definition of the FCL performance presented earlier in different non-CPW configurations [28–30].

Finally, for comparison, scattering parameter levels, the phase difference between outputs, and the even/odd mode excitation cases are restudied for the same structure with the same dielectric constant

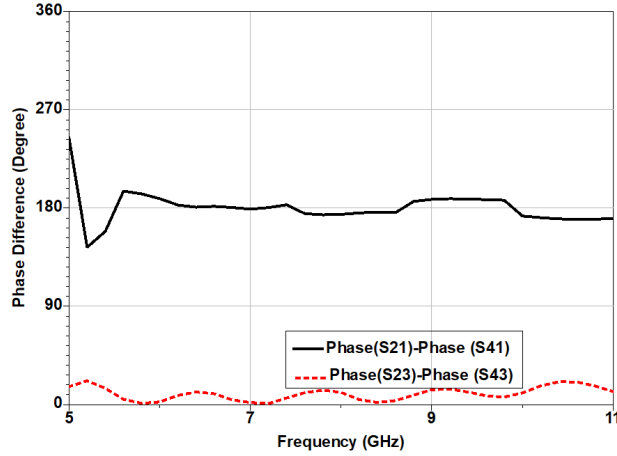


Figure 6. The full-wave simulated wrapped phase difference for two excitation cases (1) at port 1 and (2) at port 3.

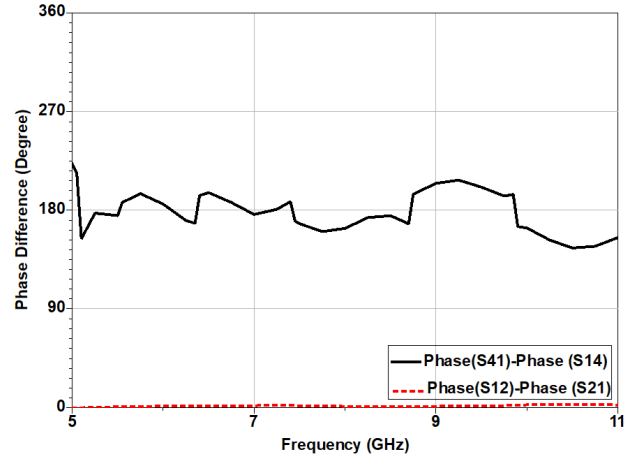


Figure 7. The full-wave simulated wrapped phase difference for the reciprocal ports (1)/(4) compared to (1)/(2).

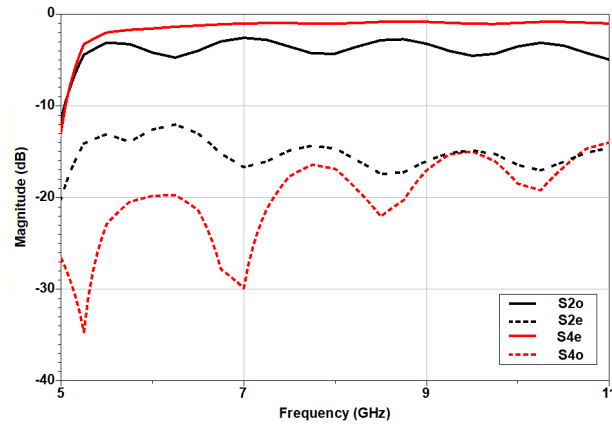


Figure 8. The full-wave simulated magnitude of scattering parameters of the CPW-FCL for even and odd excitations.

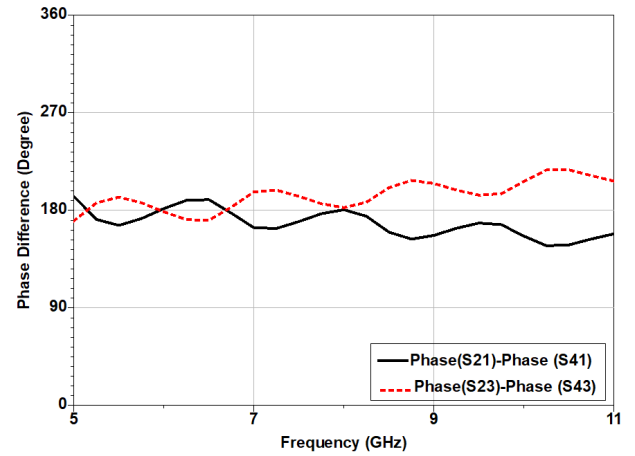


Figure 9. The full-wave simulated phase difference of scattering parameters of the CPW dielectric coupled line for the two outputs for excitations at ports 1 and 3.

instead of the ferrite substrate as shown in Fig. 9 and Fig. 10, respectively. These results completely disagree with the definition of the FCL performance. As the magnitude of output signals are equal while their phase differences are either in phase or out of phase, the CPW-FCL junction can be described as a phase nonreciprocal.

3. CPW-FCL GYRATOR

3.1. CPW-FCL Gyrator Theory

A gyrator is a twoport nonreciprocal phase device used to transmit electromagnetic waves in both directions with 180° rehearsal [4]. The scattering matrix of a gyrator is expressed as

$$[S] = \begin{bmatrix} 0 & 1 \\ -1 & 0 \end{bmatrix} \quad (8)$$

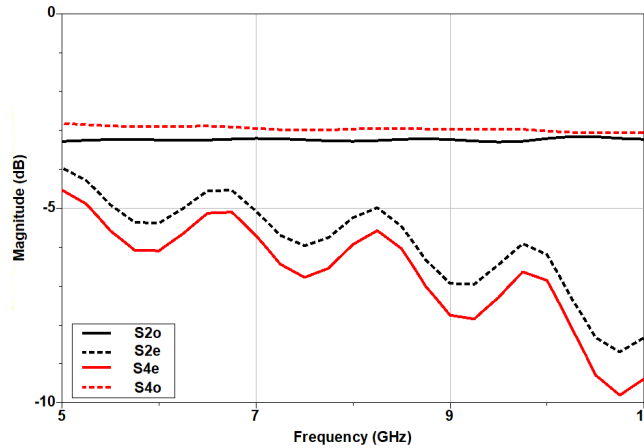


Figure 10. The full-wave simulated magnitude of scattering parameters of the CPW dielectric coupled line for the even/odd excitation cases.

As explained earlier, the FCL gyrator can be designed by connecting one pair of ports to either open or short-circuited load. In our work, the proposed CPW-FCL gyrator is designed by connecting its two ending ports, port 2 and port 4, using a plate of metal that acts as a perfect short circuit load. To show the possibility of the proposed FCL section being applied in a gyrator, the dimensions used in the CPW-FCL gyrator are the same as the optimized CPW-FCL section. However, better performance of the proposed CPW-FCL gyrator through the change of the length of the FCL section is achieved.

The performance of the proposed gyrator can be explained as follows. When the structure is excited at one port from its two adjacent starting ports, port 1 or port 3, the equally divided coupled power at the end two ports, port 2 and port 4, will be reflected in the FCL section in the form of either even/odd mode excitation, according to the first exciting port, with the reverse magnetization of the FCL section. Following the scattering matrix of the FCL section, the output power will be coupled to the second starting port, port 3 or port 1 respectively with out of phase. This agrees with the typical gyrator performance. Therefore, the grounded FCL will act as a gyrator within the frequency band of the FCL.

3.2. CPW-FCL Gyrator Simulation Results

Similar to the FCL section study, the EM simulation study of the proposed CPW-FCL gyrator has used full-wave simulation. The dimensions of the CPW-FCL gyrator are optimized with little change from the previously described CPW-FCL junction. It is worth commenting that the length of the CPW-FCL section was increased to 37 mm instead of 36 mm for better gyrator function.

The simulated magnitude of the scattering parameters of the CPW-FCL gyrator is shown in Fig. 11 while the phase of its transmission coefficients (S_{21} and S_{12}) is shown in Fig. 12.

In Fig. 11, it is clear that the two magnitudes have a periodic propagation nature, and their levels are around -2 dB for S_{21} within the frequency band from 6 GHz to 11 GHz. For S_{12} magnitude, it has a periodic nature with a peak level of approximately -5 dB at 7 GHz, 8.2 GHz, 9.3 GHz, and 10.8 GHz. Also, the return loss (magnitudes of S_{11} and S_{22}) at the operating frequency of the proposed gyrator is less than 10 dB approximately, within the frequency band from 5 GHz to 11 GHz. Moreover, the return loss is lower than 15 dB from 6.2 GHz to 11 GHz except two frequency windows: (1) from 9 GHz to 9.4 GHz, where it is 13 dB and (2) from 10.2 GHz to 10.7 GHz where it is 11 dB.

On the other hand, the phase of both transmission coefficients S_{21} and S_{12} introduces periodic nature, similar to their magnitude behavior as can be seen in Fig. 12. It can be extracted from Fig. 12 that the phase difference (Phase (S_{21})-Phase (S_{12})) is 180° at discrete frequencies (for example at 6.25 GHz, 7.25 GHz, and 8.4 GHz), within the operating frequency band of the CPW-FCL section. As a final comment, it can be claimed that the previous results agree with the typical FCL gyrator.

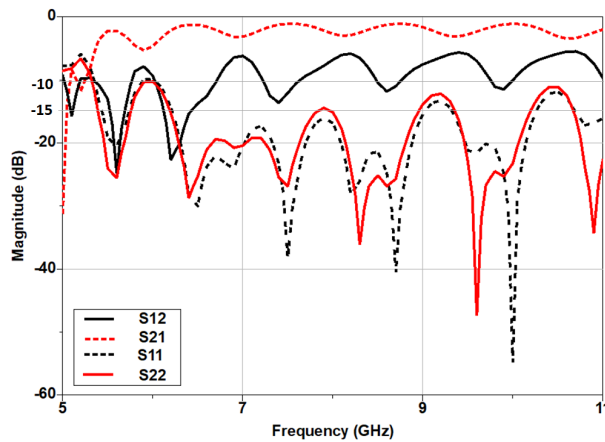


Figure 11. The full-wave simulated magnitude of scattering parameters of the CPW-FCL gyrator.

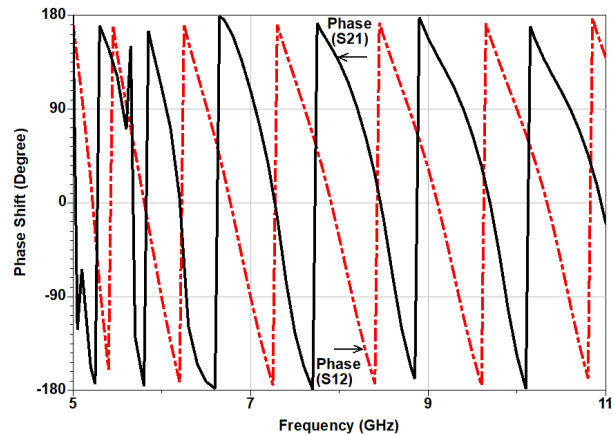


Figure 12. The full-wave simulated phase of scattering parameters of the CPW-FCL gyrator.

4. CONCLUSION

A wideband CPW ferrite coupled line has been proposed, and a new CPW-FCL gyrator is presented. The design of the CPW-FCL section is optimized using full-wave EM simulations. The simulated results have proven that the CPW-FCL section has typical magnitude and phase properties for different excitation ports. Also, the CPW-FCL response for the even and odd mode excitation within the frequency band from 5 GHz to 11 GHz is verified. Finally, a wideband CPW-FCL gyrator has been introduced as the application of the CPW-FCL section. The gyrator simulated results agree in phase and magnitude with typical gyrator function at discrete frequencies within the frequency band from 5 GHz to 11 GHz.

REFERENCES

1. Lax, B. and K. J. Buton, *Microwave Ferrites and Ferrimagnetics*, McGraw-Hill, New York, USA, 1962.
2. Fuller, A. J. B., *Ferrites at Microwave Frequencies*, Peregrinus, London, U.K., 1987.
3. Harris, V. G., "Modern microwave ferrites," *IEEE Trans. on Magn.*, Vol. 48, No. 3, 1075–1104, 2011.
4. Pozar, D. M., *Microwave Engineering*, Addison-Wesley, Reading, MA, 1990.
5. Hines, M. E., "Reciprocal and nonreciprocal modes of propagation in ferrite stripline and microstrip devices," *IEEE Trans. Microw. Th. & Tech.*, Vol. 19, No. 5, 442–451, 1971.
6. Webb, D. C., "Microwave magnetic thin-film devices," *IEEE Trans. Magn.*, Vol. 24, No. 6, 2799–2804, 1988.
7. Adam, J. D., L. E. Davis, G. F. Dionne, E. F. Schloemann, and S. N. Stitzer, "Ferrite devices and materials," *IEEE Trans. Microw. Th. & Tech.*, Vol. 50, No. 3, 721–737, 2002.
8. Geiler, A. and V. Harris, "Atom magnetism: Ferrite circulators — Past, present, and future," *IEEE Microwave Magazine*, Vol. 15, No. 6, 66–72, 2014.
9. Linkhart, D., *Microwave Circulator Design*, Artech House Microwave Library, Artech House, Norwood, MA, 1989.
10. Shams, S. I., M. Elsaadany, and A. A. Kishk, "Including stripline modes in the Y-junction circulators: Revisiting fundamentals and key design equations," *IEEE Trans. Microw. Th. & Tech.*, 67, No. 1, 94–107, 2018.

11. Hord, W. E., C. R. Boyd, and D. Diaz, "A new type of fast-switching dual-mode ferrite phase shifter," *IEEE Trans. Microw. Th. & Tech.*, Vol. 35, No. 12, 1219–1225, 1987.
12. Peng, B., H. Xu, H. Li, W. Zhang, Y. Wang, and W. Zhang, "Self-biased microstrip junction circulator based on barium ferrite thin films for monolithic microwave integrated circuits," *IEEE Trans. Magn.*, Vol. 47, No. 6, 1674–1677, 2011.
13. Wang, J., A. Yang, Y. Chen, Z. Chen, A. Geiler, S. M. Gillette, G. H. Vincent, and C. Vittoria, "Self-biased Y-junction circulator at Ku band," *IEEE Microw. Wireless Compon. Lett.*, Vol. 21, No. 6, 292–294, 2011.
14. Laur, V., G. Vérissimo, P. Quéffélec, L. A. Farhat, H. Alaaeddine, E. Laroche, G. Martin, R. Lebourgeois, and J. Ganne, "Self-biased Y-junction circulators using lanthanum-and cobalt-substituted strontium hexaferrites," *IEEE Trans. Microw. Th. & Tech.*, Vol. 63, No. 12, 4376–4381, 2015.
15. Spiegel, J., J. de la Torre, M. Darques, L. Piraux, and I. Huynen, "Permittivity model for ferromagnetic nanowired substrates," *IEEE Microw. Wireless Compon. Lett.*, Vol. 17, No. 7, 492–494, 2007.
16. Saib, A., M. Darques, L. Piraux, D. Vanhoenacker-Janvier, and I. Huynen, "An unbiased integrated microstrip circulator based on magnetic nanowired substrate," *IEEE Trans. Microw. Th. & Tech.*, Vol. 53, No. 6, 2043–2049, 2005.
17. Cheng, Y. J., Q. D. Huang, Y. R. Wang, and J. L.-W. Li, "Narrowband substrate integrated waveguide isolators," *IEEE Microw. Wireless Compon. Lett.*, 24, No. 10, 698–700, 2014.
18. Beguhn, S., X. Yang, and N. X. Sun, "Wideband ferrite substrate integrated waveguide isolator using shape anisotropy," *J. Appl. Phys.*, Vol. 115, 17E503–1–17E503–3, 2014.
19. D'Orazio, W. and K. Wu, "Substrate-integrated-waveguide circulators suitable for millimeter-wave integration," *IEEE Trans. Microw. Th. & Tech.*, Vol. 54, No. 10, 3675–3680, 2006.
20. Martinez, L., V. Laur, A. L. Borja, P. Queffelec, and A. Belenguer, "Low loss ferrite Y-junction circulator based on empty substrate integrated coaxial line at Ku-band," *IEEE Access*, Vol. 7, 104789–104796, 2019.
21. Elshafiey, T. M. F., J. T. Aberle, and E.-B. El-Sharawy, "Full wave analysis of edge-guided mode microstrip isolator," *IEEE Trans. Microw. Th. & Tech.*, Vol. 44, No. 12, 2661–2668, 1996.
22. Marynowski, W., R. Lech, and J. Mazur, "Edge-guided mode performance and applications in nonreciprocal millimeter-wave gyroelectric components," *IEEE Trans. Microw. Th. & Tech.*, Vol. 65, No. 12, 4883–4892, 2017.
23. Koshiji, K. and E. Shu, "Circulators using coplanar waveguide," *Elect. Letters*, Vol. 22, No. 19, 1000–1002, 1986.
24. Bayard, B., D. Vincent, C. R. Simovski, and G. Noyel, "Electromagnetic study of a ferrite coplanar isolator suitable for integration," *IEEE Trans. Microw. Th. & Tech.* Vol. 51, No. 7, 1809–1814, 2003.
25. Abdalla, M. A. and Z. Hu, "Composite right/left-handed coplanar waveguide ferrite forward coupled-line coupler," *IET Microw., Ant. & Propaga.*, Vol. 9, No. 10, 1104–1111, 2015.
26. Abdalla, M. A. and Z. Hu, "Reconfigurable/tunable dual band/dual mode ferrite composite right/left-handed CPW coupled-line coupler," *J. of Instrumentation*, Vol. 12, No. 9, P09009, 2017.
27. Joseph, S., R. Lebourgeois, Y. Huang, L. Roussel, and A. Schuchinsky, "Low-loss hexaferrite self-biased microstrip and CPW circulators," *Proc. in IEEE 2019 13rd Int. Congress on Artificial Materials for Novel Wave Phenomena (Metamaterials)*, X-372, 2019.
28. Davis, L. and D. B. Sillars, "Millimetric nonreciprocal coupled-slot finline components," *IEEE Trans. Microw. Th. & Tech.*, Vol. 34, No. 7, 804–808, 1986.
29. Michalski, J., M. Mazur, and J. Mazur, "Scattering in a section of ferrite-coupled microstrip lines: Theory and application in nonreciprocal devices," *IEE Proc. — Microw., Antennas and Propagation*, Vol. 149, No. 56, 286–290, 2002.
30. Yang, L.-Y. and K. Xie, "Periodically non-uniform coupled microstrip lines on longitudinally-magnetised ferrite," *Elect. Letters*, Vol. 45, No. 5, 268–270, 2009.

31. Mazur, J., M. Mazur, J. Michalski, and E. Sedek, "Isolator using a ferrite-coupled-lines gyrator," *IEE Proc. — Microw., Antennas and Propagation*, Vol. 149, No. 56, 291–294, 2002.
32. Marynowski, W., A. Kusiek, and J. Mazur, "Microstrip ferrite coupled line isolators," *Proc. Int. Conf. on Microwaves, Radar & Wireless Communications*, 342–345, 2006.
33. Mazur, J., M. Solecka, R. Poltorak, and M. Mazur, "Theoretical and experimental treatment of a microstrip coupled ferrite line circulator," *IEE Proc. — Microw., Antennas and Propagation*, Vol. 151, No. 6, 477–480, 2004.
34. Queck, C. K. and L. E. Davis, "Dually magnetised stripline ferrite coupled line (FCL) section," *Elect. Letters*, Vol. 39, No. 5, 439–440, 2003.
35. Queck, C. K., L. E. Davis, K. Xie, K. Newsome, B. Climer, and N. E. Priestley, "Performance of stripline-type ferrite coupled line circulators," *Int. J. of RF and Microw. Computer-Aided Engineering*, Vol. 13, No. 3, 173–179, 2003.
36. Queck, C. K. and L. E. Davis, "Broad-band three-port and four-port stripline ferrite coupled line circulators," *IEEE Trans. Microw. Th. & Tech.*, Vol. 52, No. 2, 625–632, 2004.
37. Kusiek, A., W. Marynowski, and J. Mazur, "Cylindrical ferrite coupled slotline junction for Faraday nonreciprocal devices," *Proc. 19th Int. Conf. on Microwaves, Radar & Wireless Communications*, 699–702, 2012.
38. Abdalla, M. A. and Z. Hu, "Ferrite-coupled coplanar waveguide," *IEEE Trans. on Magnetics*, Vol. 44, No. 11, 3099–3102, 2008.
39. Abdalla, M. A. and Z. Hu, "Compact novel CPW ferrite coupled line circulator with left-handed power divider/combiner," *Proc. 41st European Microwave Conf.*, 794–497, 2011.
40. Marynowski, W. and J. Mazur, "Investigations of multilayer three-strip coplanar lines with the ferrite material," *Proc. 18th Int. Conf. on Microwaves, Radar & Wireless Communications*, 1–3, 2010.
41. Kusiek, A., W. Marynowski, and J. Mazur, "Nonreciprocal properties of elliptical ferrite coupled line junction," *Proc. 21st Int. Conf. on Microwaves, Radar & Wireless Communications*, 1–4, 2016.
42. Marynowski, W., A. Kusiek, and J. Mazur, "Four-port circulator using reduced ground plane ferrite coupled line junction," *Proc. 8th European Conf. on Ant. & Propaga. (EuCAP 2014)*, 903–906, 2014.
43. Mazur, J. and M. Mrozowski, "On the mode coupling in longitudinally magnetized waveguiding structures," *IEEE Trans. Microw. Th. & Tech.*, Vol. 37, No. 1, 159–165, 1989.
44. Mazur, J. and M. Mrozowski, "Nonreciprocal operation of structures comprising a section of coupled ferrite lines with longitudinal magnetization," *IEEE Trans. Microw. Th. & Tech.*, Vol. 37, No. 6, 1012–1020, 1989.
45. Teoh, C. S. and L. E. Davis, "Normal-mode analysis of ferrite-coupled lines using microstrips or slotlines," *IEEE Trans. Microw. Th. & Tech.*, Vol. 43, No. 2, 2991–2998, 1995.
46. Teoh, C. S. and L. E. Davis, "Normal-mode analysis of coupled-slots with an axially-magnetized ferrite substrate," *Proc. Int. Conf. Microw. Symposium*, 99–102, May 1995, Orlando, USA.
47. Xie, K. and L. E. Davis, "Nonreciprocity and the optimum operation of ferrite coupled lines," *IEEE Trans. Microw. Th. & Tech.*, Vol. 48, No. 4, 562–573, 2000.
48. Mazur, J., M. Mazur, J. Michalski, and E. Sedek, "Development of ferrite coupled lines gyrator," *Proc. 14th Int. Conf. on Microwaves, Radar & Wireless Communications*, Vol. 1, 245–248, 2002.
49. Mazur, J., M. Mazur, J. Michalski, and E. Sedek, "Isolator using a ferrite-coupled-lines gyrator," *IEE Proc. — Microw., Antennas and Propagation*, Vol. 149, No. 56, 291–294, 2002.